GEOMOR-03067; No of Pages 15

Geomorphology xxx (2009) xxx–xxx

Contents lists available at ScienceDirect

Geomorphology

journal homepage: www.elsevier.com/locate/geomorph

The geomorphology and sedimentology of the Tista megafan, Darjeeling Himalaya: Implications for megafan building processes

Tapan Chakraborty *, Parthasarathi Ghosh

Geological Studies Unit, Indian Statistical Institute, 203 B. T. Road, Kolkata 700108, India

ARTICLE INFO

Article history:
Received 24 December 2007
Received in revised form 6 May 2009
Accepted 15 June 2009
Available online xxxx

Keywords:
Geomorphology
Megafans
Alluvial fans
Tista River
Sikkim–Darjeeling Himalaya
Himalayan Foreland

ABSTRACT

This paper reports a study of the Tista megafan in the foothills of Darjeeling Himalaya. Spread over parts of India and Bangladesh, the megafan is bounded by the Mahananda River to its west and the Tista River to the east. The Atrai and Karatoya Rivers flow through its axial part. The megafan covers an area of ~18,000 km^2. Near its apex the surface slope is ~0.19°, that declines to 0.01° near the toe. The east–west transverse profile of the megafan is broadly upward convex, with gently sloping (~0.01°) flanks. Maximum width and the length of the megafan are about 145 km and 166 km respectively. The highest point near the megafan apex is ~150 m above the Brahmaputra alluvial plain. The Tista River flanking the megafan has an average annual discharge of 609 m^3/s with highest average monthly discharge exceeding 2000 m^3/s during monsoon. Most of the other channels currently traversing the megafan are plains-fed, and compared to Tista and Mahananda Rivers these channels have lesser discharge, higher sinuosity, and decreased widths. A radiating network of abandoned channel belts can be identified in satellite images of the megafan. Each of these major paleochannels is associated with numerous crevasse channels in the distal part of the megafan, forming an intricate network of radial drainage on the megafan surface.

Three distinct depositional lobes can be recognised on the Tista megafan. Each of the lobes is identified by a set of ancient and modern radial drainage systems. The lobe boundaries are marked by discordance in drainage network of adjacent lobes. The relative ages of the lobes, as tentatively determined from the drainage discordances, indicate that the megafan first built up the eastern lobe (lobe 1), then shifted to the west to form lobe 2, and finally switched again eastward giving rise to the smallest lobe located close to the mountain front (lobe 3). Although broadly upward convex in cross profiles, subtle reflections of multiple lobes are apparent in some of the cross profiles. Study of the old maps published between 1794 and 1945 reveals that some of the present-day plains-fed rivers, like the Tangon, the Atrai and the Karatoya, were directly connected to the Himalayan catchment basins prior to the late eighteenth century. Archaeological excavations along the banks of these rivers appear to support this paleodrainage configuration. Eight facies and five facies associations were recognised in the uppermost megafan sediments. Facies associations suggest deposition from high-energy sandy streams in the proximal area and deposition from mixed load, sinuous streams and flanking marsh or lake in the distal part of the lobes. Paleocurrent data are consistent with a southwestward spreading paleochannel pattern recognised within the studied part of the megafan.

Multiple lobes typify megafans ocurring in different parts of the globe. The existence of the mutiple accretionary lobes in Tista megafan, its radial drainage pattern, its concave-upward longitudinal and convex-upward transverse profile shape make it morphologically comparable with other high-gradient alluvial fans observed in nature and those produced in the laboratory. These morphological features denote the similarities between the small, high-gradient alluvial fans and large, low-gradient megafans, and that in turn may be indicative of the commoness in certain controlling factors between these two depositional systems.

1. Introduction

The megafans are fan-shaped alluvial bodies characterised by large area (>1000 km^2), low gradient (generally <0.5°), radial drainage pattern and preponderance of fluid-gravity flow deposits (Gohain and Prakash, 1990; Sinha and Friend, 1994; Leier et al., 2005). In contrast, typical high-gradient alluvial fans are known to have smaller size (≤100 km^2), steeper gradient (>1.5°) and are dominated by sediment gravity flow, supercritical sheet flood or proximal gravelly braided river deposits (Bull, 1977; Nemec and Postma, 1993; Blair and McPherson, 1994; Leeder, 1999). Megafans have been documented from many modern foreland basins, particularly those of Andes and Himalayas

* Corresponding author. Tel.: +91 33 2575 3150 (office), +91 33 2429 2451 (home); fax: +91 33 2577 3026.
E-mail address: tapan@isical.ac.in (T. Chakraborty).

0169-555X/$ – see front matter © 2009 Elsevier B.V. All rights reserved.
doi:10.1016/j.geomorph.2009.06.035

Please cite this article as: Chakraborty, T., Ghosh, P., The geomorphology and sedimentology of the Tista megafan, Darjeeling Himalaya: Implications for megafan building processes, Geomorphology (2009), doi:10.1016/j.geomorph.2009.06.035

(Wells and Dorr, 1987; Gohain and Prakash, 1990; Iriondo, 1993; Decelles and Cavazza, 1999; Wilkinson et al., 2006). The megafan deposits have also been identified from a few ancient foreland basin alluvial successions (Willis, 1993; Lawton et al., 1994; DeCelles and Cavazza, 1999; Horton and DeCelles, 2001).

Study of the large sediment bodies of megafans flanking mountain belts is important as they preserve the record of rates and timing of tectonic activity and the climatic setting affecting the orogenic belt from which the basin-filling drainage emanates (Huyghe et al., 2001; Leier et al., 2005; Densmore et al., 2007). A number of case studies document the essential geomorphic character and sedimentation model of the megafans (Geddes, 1960; Gohain and Prakash, 1990; Singh et al., 1993; Shukla et al., 2001; Horton and DeCelles, 2001; Assine, 2005; Wilkinson et al., 2006). However, the factors controlling the development of the megafans and their mechanism of formation remain less clear (Blair and McPherson, 1994; Gupta, 1997; Whipple et al., 1998; Leier et al., 2005).

Many large megafans occur in the Indus–Ganges–Brahmaputra alluvial plain (Fig. 1). The most well-known among them is the Kosi megafan for its reported history of extremely fast westward lateral migration of its main feeder channel across the surface of the megafan over last 200 years (Mukherjea and Aich, 1963; Gole and Chitale, 1966; Wells and Dorr, 1987; Gohain and Prakash, 1990). Another, even larger megafan, east of the Kosi megafan in the same latitudinal belt, referred to as Tista megafan (DeCelles and Cavazza, 1999), has drawn much less attention from geoscientists. This paper reports geomorphologic and sedimentologic investigations of the Tista megafan and discusses its significance and implications for megafan building processes.

2. Geological setting

The Himalayan orogenic belt is flanked by a ~2000 km long foreland alluvial plain (Fig. 1). Three of the largest rivers of the world namely, the Indus, the Ganges and the Brahmaputra, and their numerous tributaries traverse this plain. The foreland basin was initiated through flexural subsidence in response to ongoing collision between the Indian and Asian continents during early Eocene time. As the thrust front migrated basinward, the older foreland sediments (mainly the Siwaliks) were deformed, exhumed and eroded and the foreland basin shifted further south (Burbank et al., 1996). Since the early Cenozoic, the drainage disposition and alluvial sedimentation patterns in the foreland were influenced by interaction between the tectonism, climate and extant basin configuration (Burbank et al., 1996; Huyghe et al., 2001; Yin, 2006; Najman, 2006). The modern foreland alluvial plain is characterised by an axial drainage flowing broadly west to east and a transverse drainage system, flowing out of the mountain belt, in a southerly direction. Sinha and Friend (1994) in a study of the rivers of the Indo-Gangetic plain, classified them into three major groups, based on the location of drainage basins with respect to the hinterland orogenic belt, the discharge and sediment load carried by them. They classified the rivers fed by the Higher Himalayan drainage basins as the mountain-fed, the rivers fed by the Lesser Himalayan drainage basins as foothill-fed and the rivers that originate in the alluvial plain, and essentially fed by rain and spring waters, were classified as plains-fed. Geddes (1960) was the first to note the occurrence of subtle but large sediment cones (his 'megacones') associated with the transverse drainages in the sub-

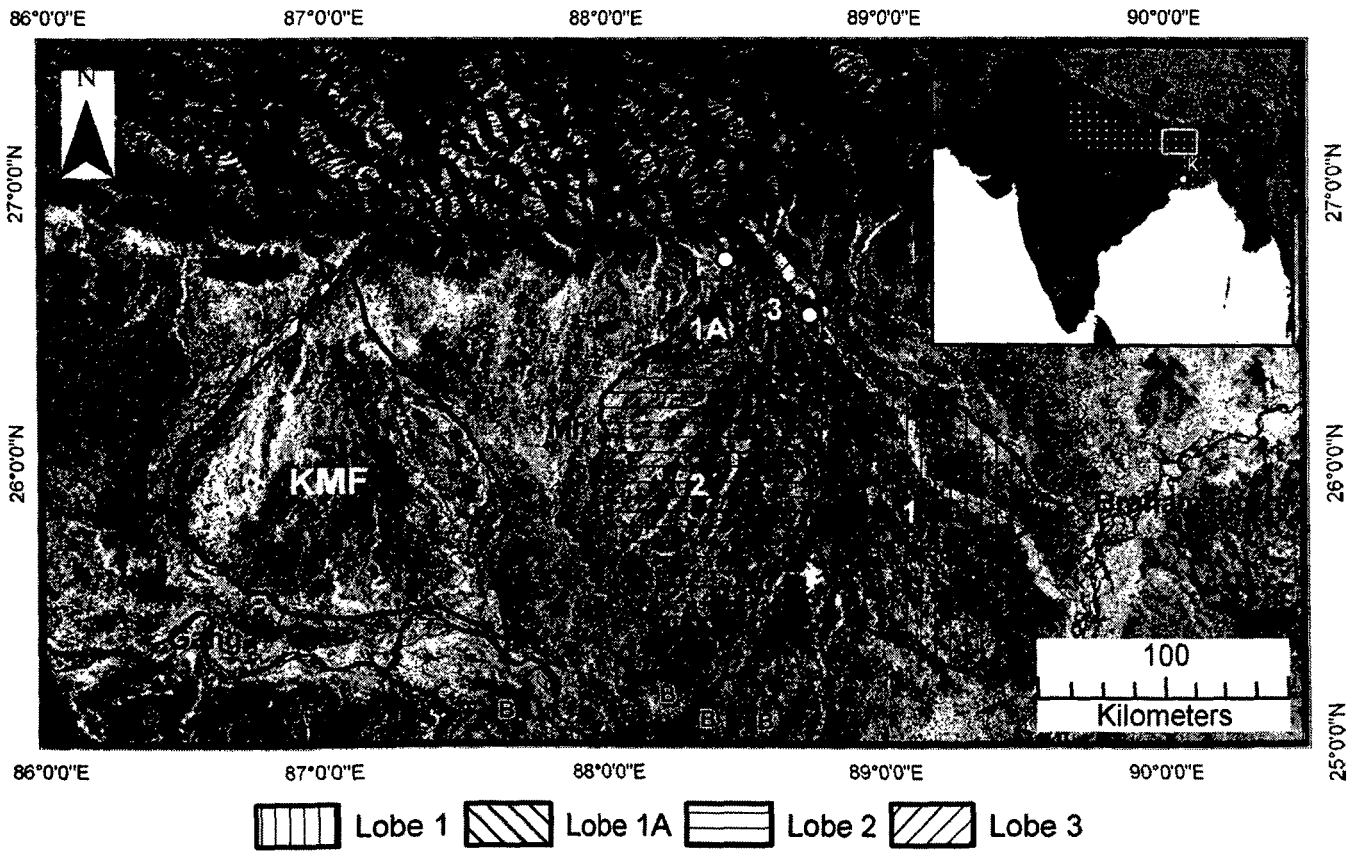

Fig. 1. A generalised map showing the Tista and Kosi megafans and the associated major drainages in the sub-Himalayan alluvial plain. Inset is a GTOPO30 view of the Himalayan orogenic belt and the flanking Ganga–Brahmaputra foreland basin (stippled). The rectangle marks the study area. 'K' in the inset marks the city of Kolkata. Note the lobes of the Tista megafan marked as 1, 1a, 2, and 3. SIL = Siliguri; JAL = Jalpaiguri; KMF = Kosi megafan; Mh = Mahananda River ; B = marks the basement spurs at the southern margin of the megafan.

Please cite this article as: Chakraborty, T., Ghosh, P., The geomorphology and sedimentology of the Tista megafan, Darjeeling Himalaya: Implications for megafan building processes, Geomorphology (2009), doi:10.1016/j.geomorph.2009.06.035

Himalayan foreland basin. These huge cone-shaped sediment bodies have subsequently been referred to as megafans (Gohain and Prakash, 1990; Sinha and Friend, 1994).

The modern foreland alluvial plain formed around 2.0 Ma in response to the uplift and folding of the Siwalik Group of rocks due to movement along Main Frontal Thrust (MFT) (Powers et al., 1998; Wesnousky et al., 1999). Quaternary sediments in the eastern Himalayan foothills unconformably overlie the Siwalik Group of rocks and older metamorphic units like Daling Group or Darjeeling Gneiss near the mountain front (Acharrya and Shastry, 1979). In the southern margin of the foreland the sediments overlie either Precambrian basement rocks or Mesozoic Rajmahal basic volcanics of the Peninsular India (Dasgupta et al., 2000).

Three distinct groups of Quaternary sediments occur in the eastern Himalayan foreland in the Darjeeling and Jalpaiguri districts of West Bengal, India. These are: (a) coarse gravely piedmont sediments lying close to the mountain front and at places extending few kilometers inside the mountain valleys; (b) pebbly, coarse to fine sand and mud related to the megafans and (c) gravel, sand and clay deposited in the modern river valleys (Shukla et al., 2001; Ghosh et al., 2005). So far there is no published age data for the Tista megafan deposits, but similar surfaces of the Ganga megafan occurring further west, have a Late Pleistocene to Holocene age (Shukla et al., 2001). In the absence of chronometric data, we have used conventional criterion like stratigraphic relationship, colour, consolidation, soil character etc. to determine the relative ages of different megafan units.

3. Geomorphology

The Tista megafan is a large triangular sediment body characterised by a radiating drainage pattern (Fig. 2). The apex of the megafan coincides with the point of emergence of Tista River from the mountain belt. The megafan spreads over India and Bangladesh covering an area of about 18,000 km^2. The megafan is bounded by the Mahananda River to the west and its eastern margin broadly coincides with the River Tista (Fig. 1). These rivers are foothills- and mountain-fed respectively (sensu Sinha and Friend, 1994). Besides the Tista and Mahananda Rivers, a large number of streams traverse the megafan. From east to west, the important modern rivers include Karatoya, Atrai, Punarbhaba, Tangon, Kulik and Nagar (Fig. 3). These rivers are plains-fed type, having significantly lower discharge compared to foothills- or hinterland-fed rivers. Satellite images display a large number of paleochannels that form a radial network on the megafan (Figs. 2 and 3).

An east–west cross profile drawn through the central part of the adjacent Kosi and Tista megafans displays convex-up shapes of both the megafan bodies (Fig. 4). Along this cross profile the Tista megafan has a

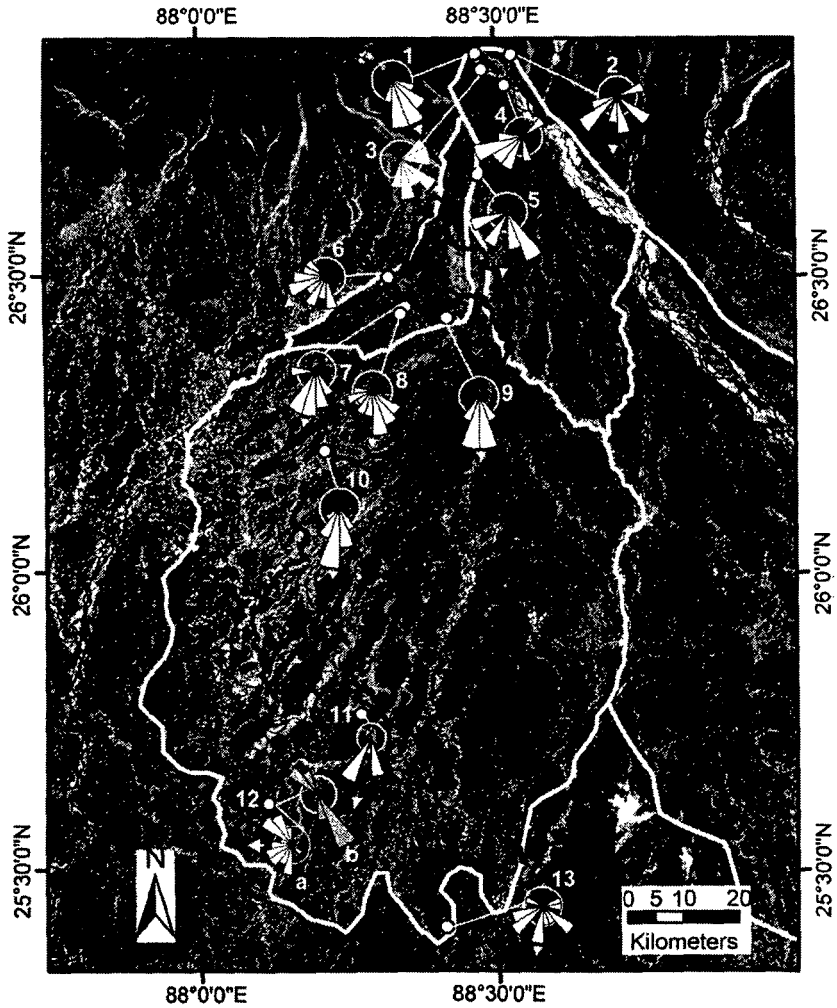

Fig. 2. Satellite image of Tista megafan. Note radiating drainage pattern of paleochannel belts on the megafan and narrower present-day plains-fed rivers. Rose diagrams, marked with 1, 2, 3 etc., show the paleoflow pattern measured from the near-surface deposits. In rose 12b, the grey coloured petals display dip data from lateral accretion surfaces ($N = 9$). White lines mark the lobes and the dark line represents the India–Bangladesh border of this area.

Please cite this article as: Chakraborty, T., Ghosh, P., The geomorphology and sedimentology of the Tista megafan, Darjeeling Himalaya: Implications for megafan building processes, Geomorphology (2009), doi:10.1016/j.geomorph.2009.06.035

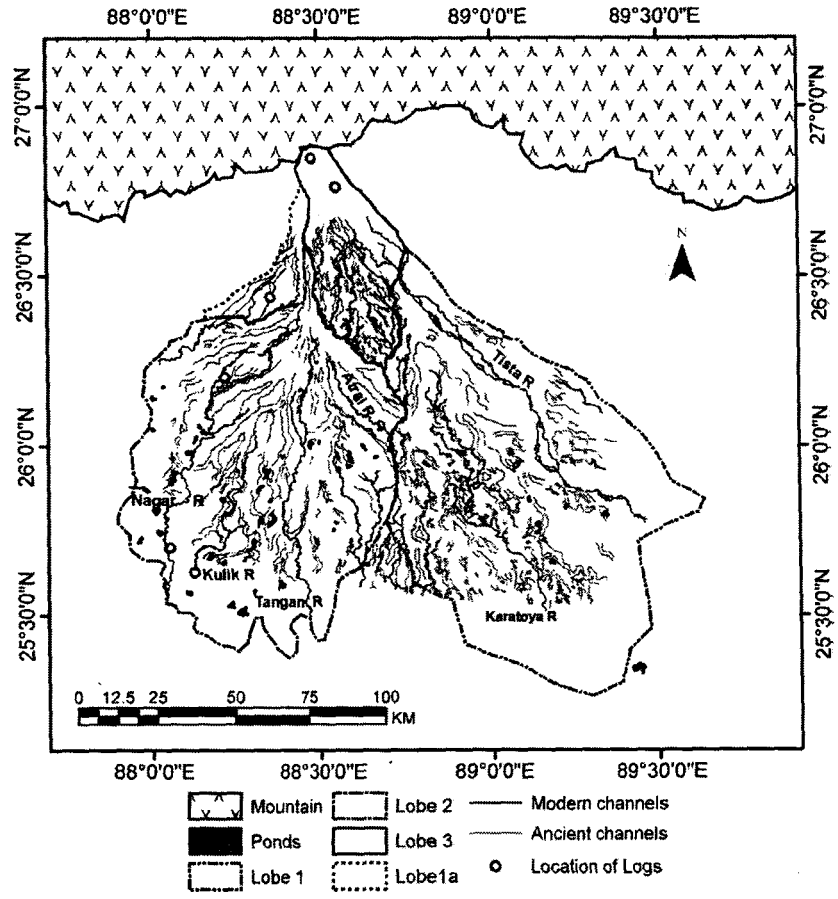

Fig. 3. Line drawing of Tista megafan showing ancient channels belts and modern channels traced from satellite images. Also shown are lobe boundaries, large marsh bodies on the megafan surfaces and the locations of sedimentological logs displayed in Fig. 8. Major plains-fed channels referred in the text are marked on the diagram.

higher elevation than the adjacent Kosi megafan, and in the map view, the Tista megafan is larger in area than the Kosi megafan (Figs. 1 and 4). The highest point of the Tista megafan is more than 150 m above the Brahmaputra alluvial plain. Highest slope of the megafan surface observed near its apex is about 0.19° that declines to 0.01° near its toe and the average slope calculated over the entire length of the megafan is about 0.05° (Fig. 4). The east–west oriented transverse profiles show that the eastern flank of the megafan is steeper than its western flank and the maximum cross profile slope is about 0.01° (Fig. 4). In a series of cross profiles drawn from north to south, the megafan shows progressive decrease in elevation and increase in width towards south (Fig. 4). Although broadly convex upward in transverse profile, the Tista megafan surface is more complex and shows multiple, convex-upward segments in some of these profiles (Fig. 4). All the longitudinal profiles are concave-up, similar to fluvial fans (cf., Whipple et al., 1998; Densmore et al., 2007).

The gauge station at Anderson Bridge, located nearly 75 km downstream of the point of exit of the Tista River from the mountain front, documents the average annual discharge between 1965 and 1971 as about 609 m^3/s (http://www.sage.wisc.edu/riverdata/scripts/station_table.php?qual=32&filenum=2567). Average monthly discharges during monsoon months exceed 2000 m^3/s (Basu and Sarkar, 1990). It has been estimated that peak discharge in Tista during 1968 devastating flood of Jalpaiguri Town, ~45 km downstream of the mountain front (Fig. 1) exceeded 19,000 m^3/s (http://www.kalpavriksh.org/f1/f1.3/ed%20ecologist%20folder/Teesta-KalyanRudra.doc). In comparison, observed peak discharge in the Punarbhaba, one of the plains-fed rivers, is reported to be about 850 m^3/s in South Dinajpur District of West Bengal, India (http://ddinajpur.nic.in/Flood_Management/flood_management.html).

The modern plains-fed rivers that traverse the megafan have a higher sinuosity and lower width as compared to the paleochannels visible in the satellite images (Figs. 2 and 3). The sinuosity of modern channels varies from 1.05 to >3.5, whereas that of the ancient channels vary from 1.49 to 1.11 and have a mean value slightly greater than 1.1. The width of the abandoned paleochannels on Tista megafan ranges between 0.1 and 3.3 km with a mean of ~1 km. The present-day plains-fed channels vary in width from 30 to 250 m (Fig. 5). There is a noticeable increase in sinuosity of both modern and ancient channels down the megafan (Figs. 2 and 3). Most of the plains-fed modern rivers are entrenched within the megafan surface and many of them are underfit relative to the existing channel morphology (Fig. 6A, B). In contrast, the wider paleochannels in places show relict mid-channel bars, and the branching-rejoining patterns that characterise braided river tracts (Fig. 6A).

One of the remarkable features of the Tista megafan is its multi-lobate character (Figs. 2 and 3). In plan, each of the lobes is characterised by a radial drainage pattern and is clearly identified by discordance of channel patterns in adjacent lobes (Figs. 2, 3, and 6D). In some of the cross profiles this multi-lobate character is discernable in the form of laterally stacked multiple convex-up segments (Profiles Tpf 1 and 2, Fig. 4). The smallest lobe, lobe 3, occurs at the northern margin of the megafan body whereas lobes 1 and 2 occur in the southern part. An isolated, small lobe in the northwestern corner of the megafan has been marked as lobe 1a (Figs. 2 and 3). The apex of radiating paleochannels of lobe 2, the most prominent lobe seen in satellite images, lies about 40 km south of the present-day mountain front as feeder system incises through lobe 1a (Figs. 2 and 3). Each of the trunk channels in the megafan is associated with a number crevasse channels in their downstream part developing an anastomosing

Please cite this article as: Chakraborty, T., Ghosh, P., The geomorphology and sedimentology of the Tista megafan, Darjeeling Himalaya: Implications for megafan building processes, Geomorphology (2009), doi:10.1016/j.geomorph.2009.06.035

network. The radially disposed trunk channels and their crevasse channels combine to produce a maze of channels on the megafan surface (Fig. 2).

The greater width and decreased sinuosity of the paleochannels seen on the megafan surface, and existence of relict braided channel patterns in some of them, indicate that wider braided streams with greater discharges and sediment loads were once active on the megafan. The widths and plan form of some of the paleochannels are comparable to the modern Mahananda or Tista Rivers. The relatively narrow, more sinuous, incised and underfit nature of the modern plains-fed channels imply lower discharge and reduced sediment loads in these channels (cf. Sinha and Friend, 1994). It is evident that the part of the megafan showing the braided paleochannels accreted in a period when larger channels forming a radiating network traversed the fan. These channels are now abandoned. The modern plains-fed channels occupy a small part of the abandoned channel tracts and are passively reworking the surface of the megafan rather than actively building it (Fig. 6A, C). The truncating relationship of the channels observed in satellite images (Fig. 6D) and elevations observed in cross profiles derived from DEM (Fig. 4e) appears to indicate that lobe 3 overlies the other lobes and is probably the youngest one. The lobe 2 drainages cut across the drainages of lobe 1 and lobe 1a implying lobe 2 to be relatively younger than lobes 1 and 1a. Lobe 1a of the megafan, though older than lobe 2, its temporal relationship with lobe 1 cannot be directly established.

The Tista megafan surface, as compared to alluvial fans, has a very gentle slope (<0.19° or 0.0033). However, convex-up cross profile and concave-up radial profile of the megafan resemble many fluvial fans (Nemec and Postma, 1993; Whipple et al., 1998; Densmore et al., 2007). Existence of radial lobes on the megafan surface resembles similar features observed in typical high-gradient alluvial fans (Bull, 1977) as well as those reported from some of the modern deep-sea fans (Damuth et al., 1988). Similar multi-lobate form is also present in model fans produced in the laboratory (Whipple et al., 1998) or those developed through numerical simulations (Densmore et al., 2007). Multi-lobate geometry of megafans, as in Tista megafan, is also evident in a number of other megafans including Taquari megafan of Brazil (Assine, 2005), Rio Pilcomayo megafan of Argentina (Horton and DeCelles, 2001; Wilkinson et al., 2006) and Zambezi megafan spread over Zambia and Angola as observed in landsat images.

3.1. Historical maps and the changing drainage of the area

We examined a number of historical maps of this area published between 1794 and 1945 and compared them to recent satellite images to understand the possible nature of changes in drainage on the megafan over the historical period. For the purpose of comparison, all maps were converted to a common geodetic map projection that uses WGS 84 datum. Due to inherent errors in these maps, comparisons are not always accurate, although several important features are clear: A radiating channel pattern comprising (from west to east) the Tangan, Atrai, and Karatoya on the megafan has been shown prominently in all these maps (Fig. 7). Many of the maps published prior to the late eighteenth or early part of the nineteenth century, show that this radiating drainage was directly connected to hinterland catchment basins of the Darjeeling–Sikkim Himalaya (Fig. 7; Rennel, 1794; Arrowsmith, 1804; Carry, 1811). In a number of these maps published prior to the mid nineteenth century the present-day course of Tista River has been shown as a small plains-fed channel draining into the Brahmaputra River (Fig. 7; see also Bristow, 1999, his Fig. 1). These maps show that rivers of the radiating network comprising the Tangan, Punarbhaba, Atrai and Karatoya were tributary to the Ganges rather than the Brahmaputra River. The maps published after the middle of the nineteenth century on the other hand, show the hinterland catchments of Darjeeling–Sikkim Himalaya to be draining through the present-day course of the Tista into the Brahmaputra River. In these later maps radiating drainage comprising the Tangan, Atrai and Karatoya is shown as plains-fed, not connected to the Himalayans catchment basins (Arrowsmith, 1844; Radefeld, 1860; Edinburgh Geographical Institute, 1893; Survey of India, 1917; 1924; Fig. 7). Some of the maps of late nineteenth century indicate increasing importance of the modern course of Tista at the cost of Tangon or Purnarbhaba (Arrowsmith, 1844; Radefeld, 1860). The Mahananda River has occupied more or less the same position in various maps since the late eighteenth century albeit there was a minor shift to the west during this period.

Archaeological sites recording remnants of ancient human settlements are common in this area (Hunter, 1876; Goswami, 1948; Ray, 1980; Chakrabarti, 2001). It appears from the historical as well as archaeological records that during the entire period of 3rd Century BC to 11th Century AD, all the courses of the radiating network of Karatoya–Atrai–Punarbhaba–Tangon Rivers existed as large navigable channels. It has been reported that in a major flood in 1787 the hinterland drainage outlet avulsed into the present-day course of River Tista abandoning the network of Tangan–Atrai–Karatoya (Hunter, 1876; Ray, 1980). This description tallies well with the observation from old maps. In tandem with the historical account of Hunter (1876), most of the maps published around or after 1850 show upland Himalayan catchment to feed Brahmaputra River through the course of present-day Tista. Evolution of the drainage pattern outlined above suggests that the radiating drainage system comprising Karatoya–Atrai–Punarbhaba–Tangon fed by the Himalayan catchment was probably responsible for aggradation of a part of the Tista megafan. Some of the wide, braided paleochannels recognised on the megafan are probably the record old drainage systems. The present-day narrow, sinuous, underfit and incised nature of many of these river channels is probably the result of decreased sediment and water discharge after their detachment from the Himalayan catchment.

4. Sedimentology

Sedimentation pattern of Tista megafan was studied in 6–35 m thick riverbank sections of some of the incised channels. The representative lithologs of the studied sections are given in Fig. 8. Since the fieldwork was confined within Indian part of the megafan, a large part of lobe 1 and lobe 2, lying within Bangladesh, could not be studied (see Fig. 2). Detail investigation of the sedimentology of the megafan is beyond the scope of this publication and the following section deals with the first order features of sedimentary facies of the Tista megafan deposits. We particularly emphasise on the proximal–distal relationship in the megafan sediments as observed in lobes 1a, 2 and 3. Eight major facies were defined following the scheme suggested by Miall (1996) in the near-surface deposit of the Tista megafan, and is summarised in Table 1. These facies have been grouped into five major facies associations (Table 2). Main attributes of each facies associations and the inferred environments are discussed in the following section.

4.1. TFA 1

The facies association is well-developed in the proximal part of lobes 1a, 2, and 3, and comprises dominantly of planar, horizontal to low-angle stratified sand (Sh, Fig. 9A). 50–90 cm thick units of this association usually begin with basal erosion surface strewn with coarse to pebbly sand and mudclasts (Ss). The erosion surfaces are overlain by sets of horizontal or low-angle stratification, which in turn grade upwards into beds of silt and clay-rich very fine sand (Fsm). At places, up to 15 cm thick shallow scour-fills of medium to coarse sand occur at the top of these units (Fig. 9A). Locally, planar cross sets with sigmoidal foresets (Sp), up to 50 cm thick, occur in pebbly sand layers. The individual sets of horizontal strata can be traced laterally for >15 m and the individual small-scale fining upward units extend several tens of meters across the entire outcrop. In the Tista River section (lobe 3), this association exposed in a 35 m river bank cliff, shows a distinct coarsening-upward trend as parallel and cross-stratified pebbly coarse sand and sandy gravel dominate the top-most part of the section (log A, Figs. 8 and 9B). Measurements from associated cross-strata in lobe 3 exposures show

Please cite this article as: Chakraborty, T., Ghosh, P., The geomorphology and sedimentology of the Tista megafan, Darjeeling Himalaya: Implications for megafan building processes, Geomorphology (2009), doi:10.1016/j.geomorph.2009.06.035

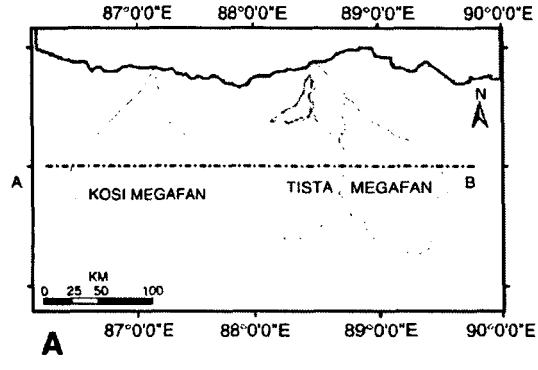

A

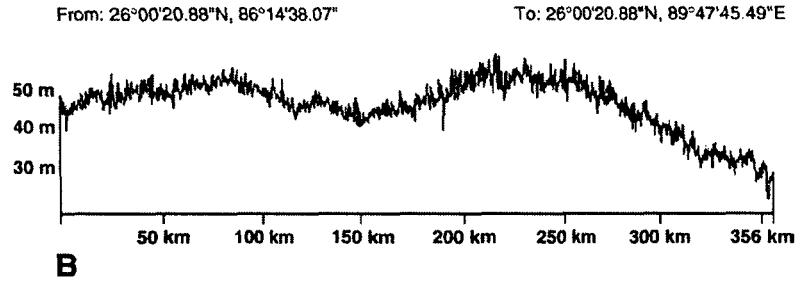

B

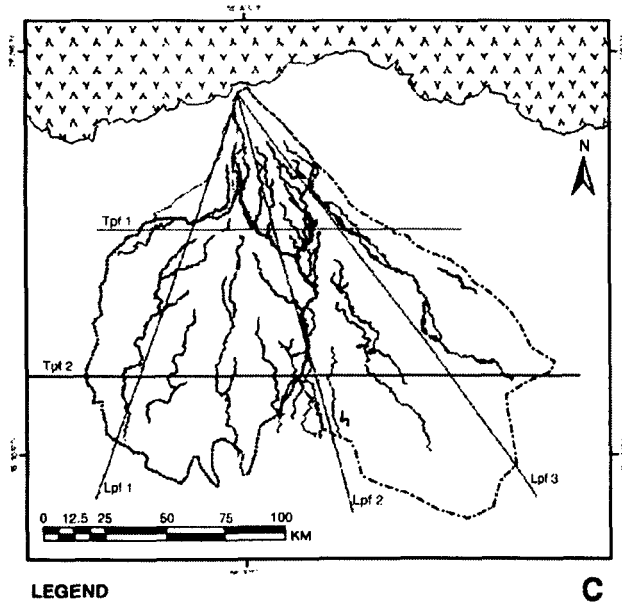

C

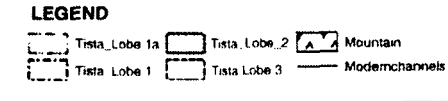

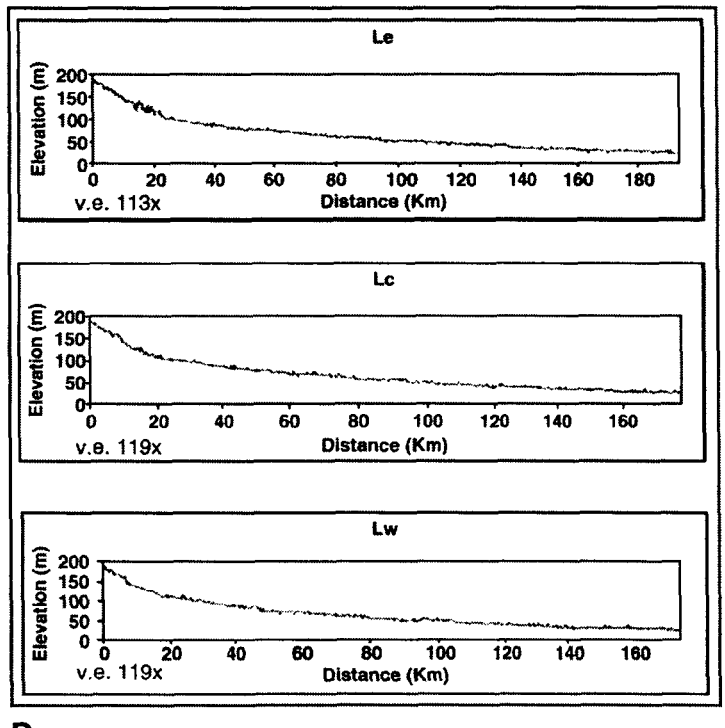

D

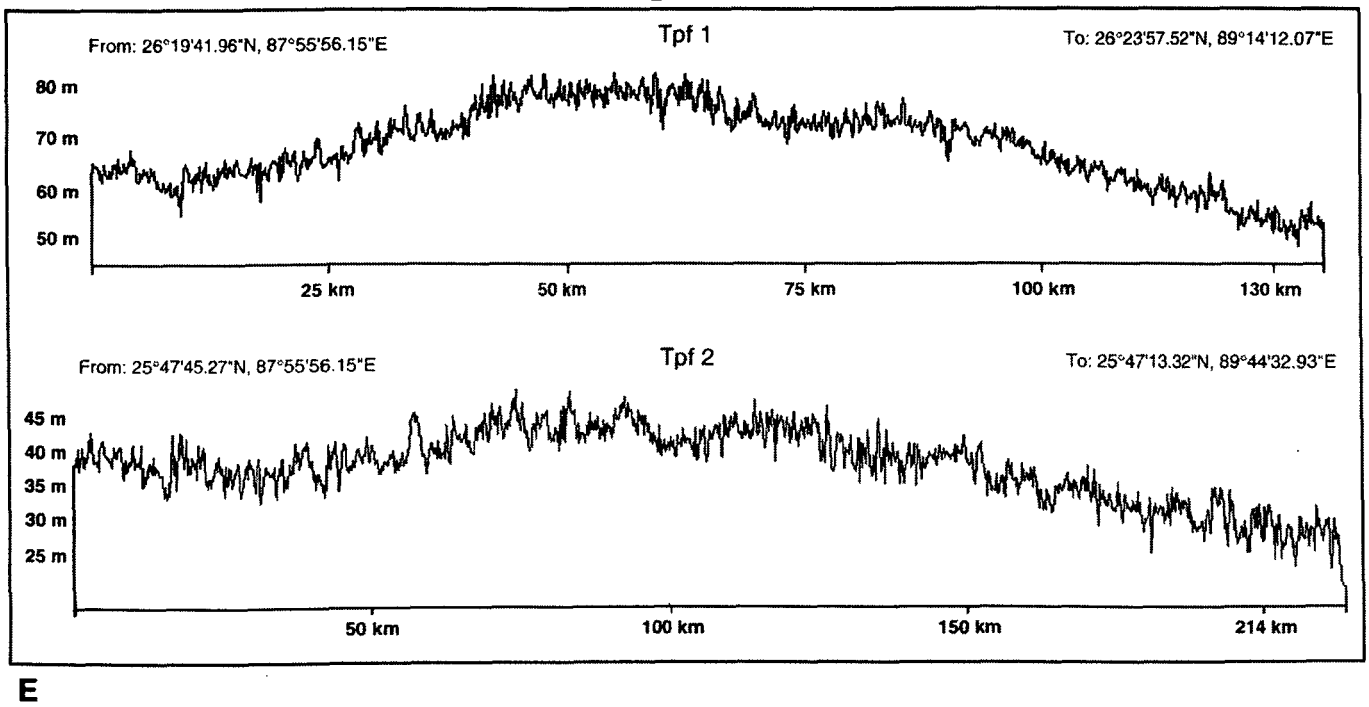

E

Please cite this article as: Chakraborty, T., Ghosh, P., The geomorphology and sedimentology of the Tista megafan, Darjeeling Himalaya: Implications for megafan building processes, Geomorphology (2009), doi:10.1016/j.geomorph.2009.06.035

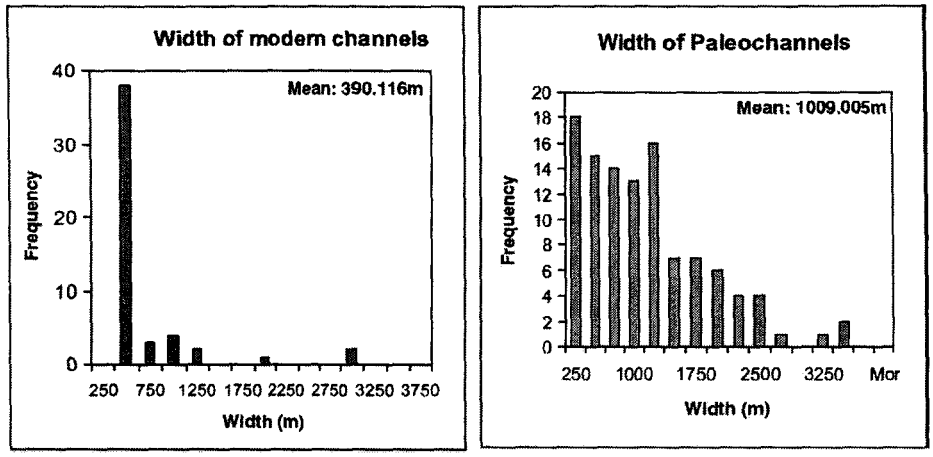

Fig. 5. Histogram showing the widths of the modern plains-fed channels and paleochannels seen on the satellite images (see Fig. 2).

paleocurrent, varying between southwest and southeast (rose 2, 3, 5, Fig. 2).

We infer the 50–90 cm thick, fining upward units to represent the product of a system of unconfined, high-energy sandy streams characterised by flashy flood discharge and rapidly decelerating flow. Overwhelming dominance of parallel stratification indicates both high flow velocity as well as availability of sandy sediments. The shallow channel fills at the top of individual units formed during low-stage flow, as decelerating sheet flow collected into few shallow channels/reels. McKee et al. (1967) and Tunbridge (1981) respectively, have documented typical modern and ancient examples of this type of sheet-braided sandy stream deposits. The planar cross-strata with sigmoidal foresets probably denote local development of humpback dunes or simple cross-stratified bars that formed under flow condition transitional to upper-phase plane beds (Saunderson and Lockett, 1983; Allen, 1983; Fielding, 2006). The distinct coarsening-upwards trend, as noted in the proximal part of lobe 3, appears to be linked to the progradation of the megafan lobe. The paleoflow pattern is consistent with a southward radiating paleochannel network.

4.2. TFA 2

The association occurs in the distal or marginal part of lobe 3 and comprises 1–3 m thick parallel and small cross-stratified medium to fine sand (St, Sh) alternating with 1.2–2 m thick dark clay–silt heterolithic layers (Fsm; log b, Fig. 8). At places dark brown to black peat layers, 10–20 cm thick, occur below the silt–clay units. Wave or combined flow ripples are common in silt layers; and small trough cross-strata of sand units measured from the downstream or lateral part of lobe 3 show mean paleoflow towards 233° and towards 152 ° (rose 4 and 1, Fig. 2).

Abundance of trough cross-strata compared to the dominance of horizontal strata in TFA1, indicates flow deceleration in the distal or marginal parts of lobe 3. Silt–clay heterolith and peat layers represent the development of marshy environment in the distal part of the sheet-braided streams of TFA 1. Wave ripples formed in the standing water body of marshes and thick vegetal growth resulted in peat and carbonaceous clay layers. The facies association is inferred to indicate low-gradient alluvial plain typified by gentler flowing streams and flanking marshes.

4.3. TFA3

The facies association comprises stacked, 1–1.5 m thick, trough and planar cross-stratified (Sp, St) pebbly coarse sand and horizontally stratified medium sand (Sh) units (Fig. 8). The facies common in the medial part of lobes 1a and 2 (Fig. 8, logs C and D). Usually 10–15 cm thick pebbly sand occurs associated with erosive base of each of the units (Ss). Parallel-stratified sandy gravels (Gh), up to 35 cm thick, also occur locally in the basal part of the facies association. In most of the exposures 5–20 cm thick trough cross-strata is the dominant structure. Half-a-meter-scale planar cross-strata and soft sediment deformations are observed at places. The sand is grey to yellowish brown with dark ferruginous blotches. Individual sand bodies of this association can be laterally traced for more than hundred meters without perceptible change in their thickness (Figs. 6B and 9C). The sand bodies generally lack fining upwards grain size trend, although some of the exposures display poorly developed fining upwards trend. In a few outcrops, a sharp contact separates sand units from over- or underlying, up to 2 m thick, red or grey clay/mud units (Fsm, Fpr).

Coarser grain size (as compared to TFA1 and TFA4), tabular geometry of the sand bodies, absence or poorly developed fining upwards grain size trend within sand bodies, locally developed basal gravelly units, and absence of lateral accretion surfaces possibly indicate deposition from low-sinuosity streams capable of carrying gravelly or coarse sandy load during flood stage. This interpretation is consistent with remnant braided bars recognised in the paleochannels seen in the satellite images in the proximal part of lobe 2 (Fig. 6A). The sharp contact of sand bodies with over- or underlying fines is inferred to result from rapid channel abandonment (Collinson, 1996). Grey or deep brown mud with iron-rich nodules represents floodplain deposits and soil development in the over bank areas of the sandy, low-sinuosity streams (cf. Bentham et al., 1993).

4.4. TFA 4

This facies association comprises 1.5–3 m thick fining upward units with well-developed Inclined Heterolithic Strata (IHS; Fig. 8, log F; Fig. 9D). This facies association is common in the distal part of lobe 2. The hereolithic strata comprise an alternation of 7–32 cm thick trough cross-stratified fine to medium sand (St) and 3–11 cm thick red mud/clay layers. The sand bed thickness decreases upwards in the

Fig. 4. a: Diagram showing the outline of Tista and Kosi megafans and location of the line of transverse profile (line A–B) as shown in b. b. Cross profiles drawn through Kosi and Tista megafans from SRTM data. Along the profile line, the highest point of the Tista megafan is at higher elevation than the Kosi megafan. c. Outline diagram showing the modern channels and lobes on the Tista megafan, and the lines of transverse (Tpf 1 and Tpf2) and longitudinal (Le, Lc, Lw) profiles shown in d. d. Three longitudinal profiles along the east, centre and west of the megafan. Note high vertical exaggeration due to low overall slope. e. Two transverse profiles across the Tista megafan. Note laterally stacked, smaller, convex-up segments in the cross profile superposed on a broad convex-up megafan surface.

Please cite this article as: Chakraborty, T., Ghosh, P., The geomorphology and sedimentology of the Tista megafan, Darjeeling Himalaya: Implications for megafan building processes, Geomorphology (2009), doi:10.1016/j.geomorph.2009.06.035

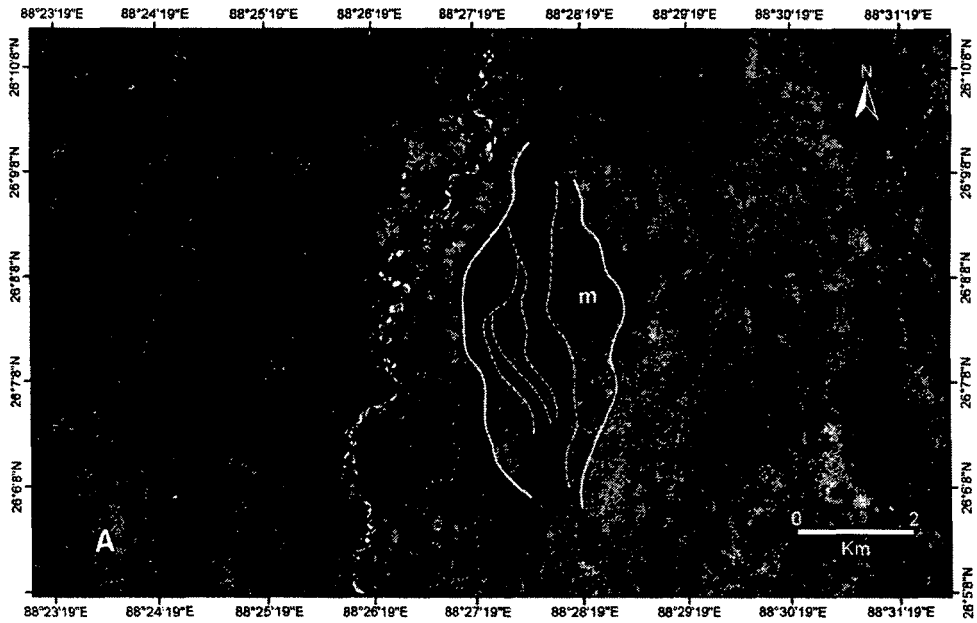

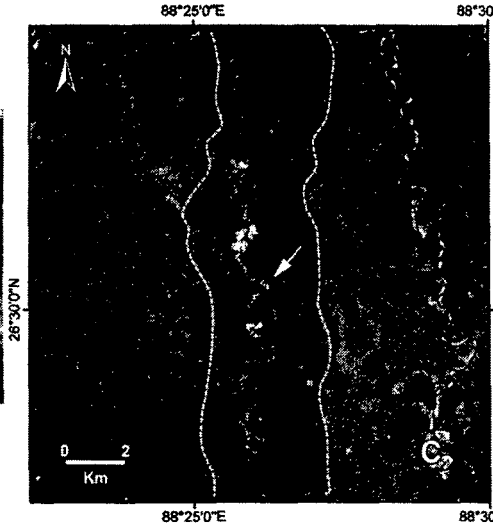

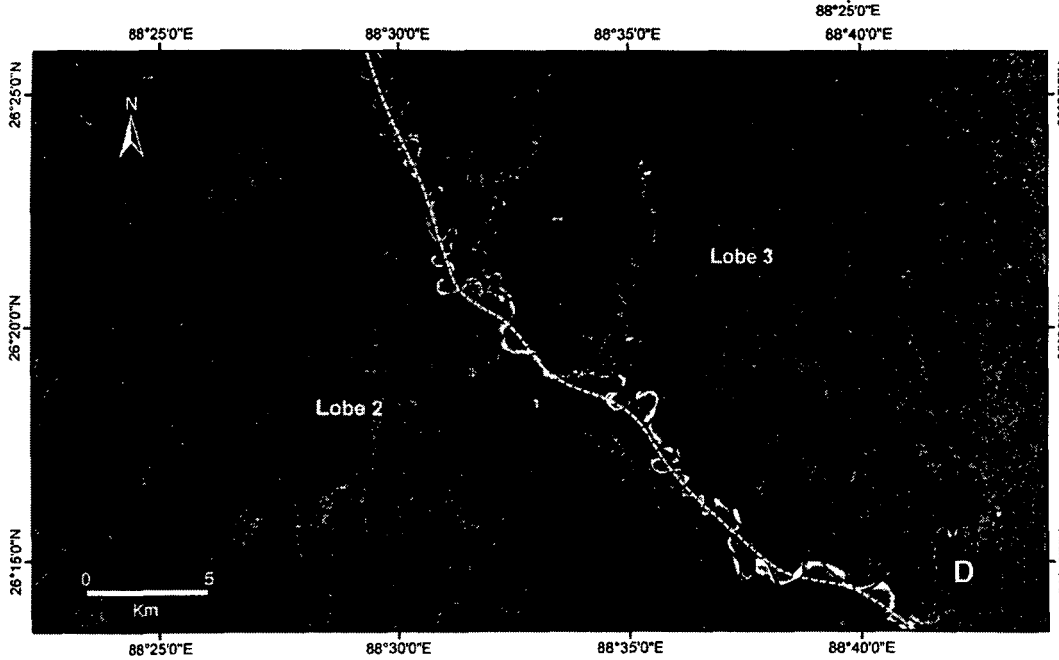

Please cite this article as: Chakraborty, T., Ghosh, P., The geomorphology and sedimentology of the Tista megafan, Darjeeling Himalaya: Implications for megafan building processes, Geomorphology (2009), doi:10.1016/j.geomorph.2009.06.035

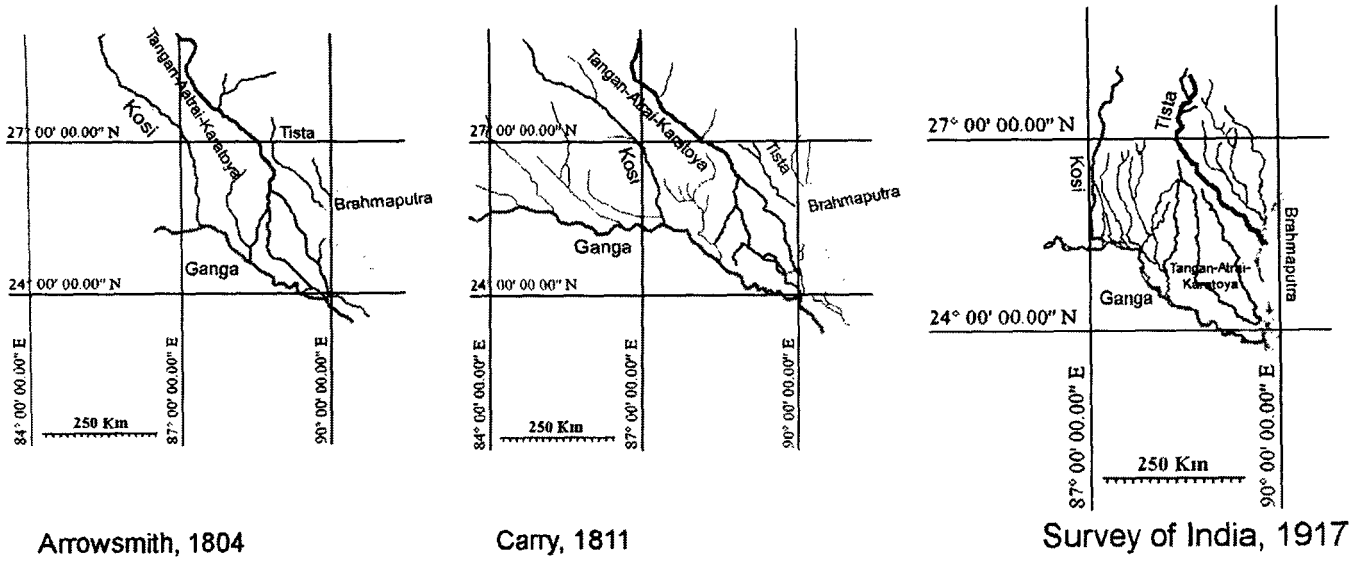

Fig. 7. Major drainages traced from three old maps. Arrowsmith, 1804: Tangan–Atrai–Karatoya directly connected to the Himalayan catchments and draining into Ganges. Note plains-fed nature of Tista River occurring as a small tributary of Brahmaputra; Carry (1811): Tangan–Atrai–Karatoya trio hinterland-fed. Note hinterland-fed Kosi and plains-fed Tista Rivers; Survey of India (1917): hinterland-fed Tista and plains-fed Tangan–Atrai–Karatoya.

units with concomitant increase of fines. Overall flow directions measured from trough cross-strata of the sand layers are towards 269° whereas the inclined surfaces (IHS) dip either to the north-northwest or to the south-southeast (rose 12a, b). The IHS units are overlain in some sections by 1.5 m thick iron nodule rich red mud or thinly layered grey mud (Fsm. Fpr; Fig. 8, log F).

High angle relationship between the mean flow direction measured from trough cross-strata and dip of the inclined heterolithic strata identifies these features as lateral accretion architectural elements (sensu Miall, 1996). Overall finer grain size and increased proportion of mud in this facies association together with well-developed fining upward trend and presence of lateral accretion elements indicate deposition of this association from mixed-load meandering streams (Collinson, 1996; Rajchl and Ulycny, 2005).

4.5. TFA 5

This facies association is characterised by up to 2.5 m thick units of dark grey, carbonaceous mud with interlayered clayey silt layers (Fsm, Fpr; Fig. 8E). Brick kiln pits, common in the distal part of lobe 2, expose large, three-dimensional bodies of this facies. Tabular, 30–70 cm thick, clayey silt beds of TFA 5, are internally rippled, have a sharp base and can be traced laterally for few hundred meters. Within this clay-dominated facies association, there are at least three 15–25 cm thick zones that show intense root turbation and iron-encrusted root moulds (Fig. 9E).

Grey colour and carbonaceous nature of the fine-grained units indicate their accumulation in an area of shallow water table and abundant vegetation typical of mashes in the flood plains of the distal part of the megafans (cf. Gohain and Prakash, 1990; Horton and DeCelles, 2001). The tabular rippled clayey silt beds probably represent crevasse lobes encroaching into these floodplain lakes (cf. Perez-Arlucia and Smith, 1999). The iron-encrusted root-beds imply the development of gleyed paleosol (Duchaufour, 1982). Three-dimensional extent of these clay-dominated units, as could be assessed from the brickfield quarries, indicates large spatial extent of these marshes. In the satellite images, recognition of large wetlands in the distal part of the Tista megafan is consistent with the occurrences of extensive units of TFA 5 in the distal part of lobe 2.

In Fig. 2, rose diagrams superposed on a mosaic of satellite images show the paleodispersal pattern documented from the near-surface Tista megafan deposits of the study area. A radiating southward paleocurrent pattern is evident in lobe 3. A south-to-southwesterly paleoflow recorded from lobes 1a and 2 is consistent with the observed south to southwesterly radiating paleochannels of the study area.

Thus, generalised facies character of the near-surface exposures studied in lobes 1a, 2 and 3 of the Tista megafan is typified by the proximal–distal transition from proximal deposits of sandy sheet-braided streams to mixed-load, low-energy, sinuous channel deposits and associated floodplain marsh deposits in the distal part of the megafan. Braided river deposits of TFA 3 with uncommon but thick over bank fines and soils typify intermediate part of the megafan (log D, Fig. 8). However, we could not map the regional distribution of the facies as large part of the megafan occurs within Bangladesh and has not been studied. Further, the paleo-marsh deposits of TFA 5, is likely to be patchy and difficult to map with limited outcrops. However, the first order features noted in the studied exposure are consistent with the observed geomorphic features of the megafan. Radial to southwestward diverging paleocurrent pattern is consistent with paleochannel traces seen in the study area and the radiating pattern reflects the convex-upward three-dimensional morphology of the megafan. The changes in the channel type and reduction in the grain size of the sediments show decreasing transport efficiency of the channels down the megafan and it appears to be the response to the southward decrease in the gradient of the megafan surface. The coarsening-upward trend of the deposits in the proximal part of lobe 3 possibly indicates progradation of the fan lobe. Similar facies pattern has been reported from the modern and ancient megafan deposits (Singh et al., 1993; Horton and DeCelles, 2001; Shukla et al., 2001). In contrast to

Fig. 6. A. Satellite image showing the close-up of abandoned channel belts on the proximal part of lobe2. Note braided pattern of the channels and a mid-channel bar (m) recognisable on the image. Note narrow, highly sinuous modern plains-fed channels on the left side of the mid-channel bar. IRS PAN Image. B. Field photograph showing entrenched Berang River (26°26′27.76″N; 88°21′19.87″E) in lobe 1a. Note about 10 m of incision of the modern Berang River. Amalgamated sheet-like sand bodies occur in the bank, the details shown in Fig. 9C. C. Underfit modern stream (arrowed) occupies the central position of a paleochannel belt (dashed lines) on the lobe 2. D. Contact between lobe 2 and lobe 3 of the Tista megafan. Note drainage discordance across the separating channel between two adjacent lobes. Dotted line marks the boundary between the lobes.

Please cite this article as: Chakraborty, T., Ghosh, P., The geomorphology and sedimentology of the Tista megafan, Darjeeling Himalaya: Implications for megafan building processes, Geomorphology (2009), doi:10.1016/j.geomorph.2009.06.035

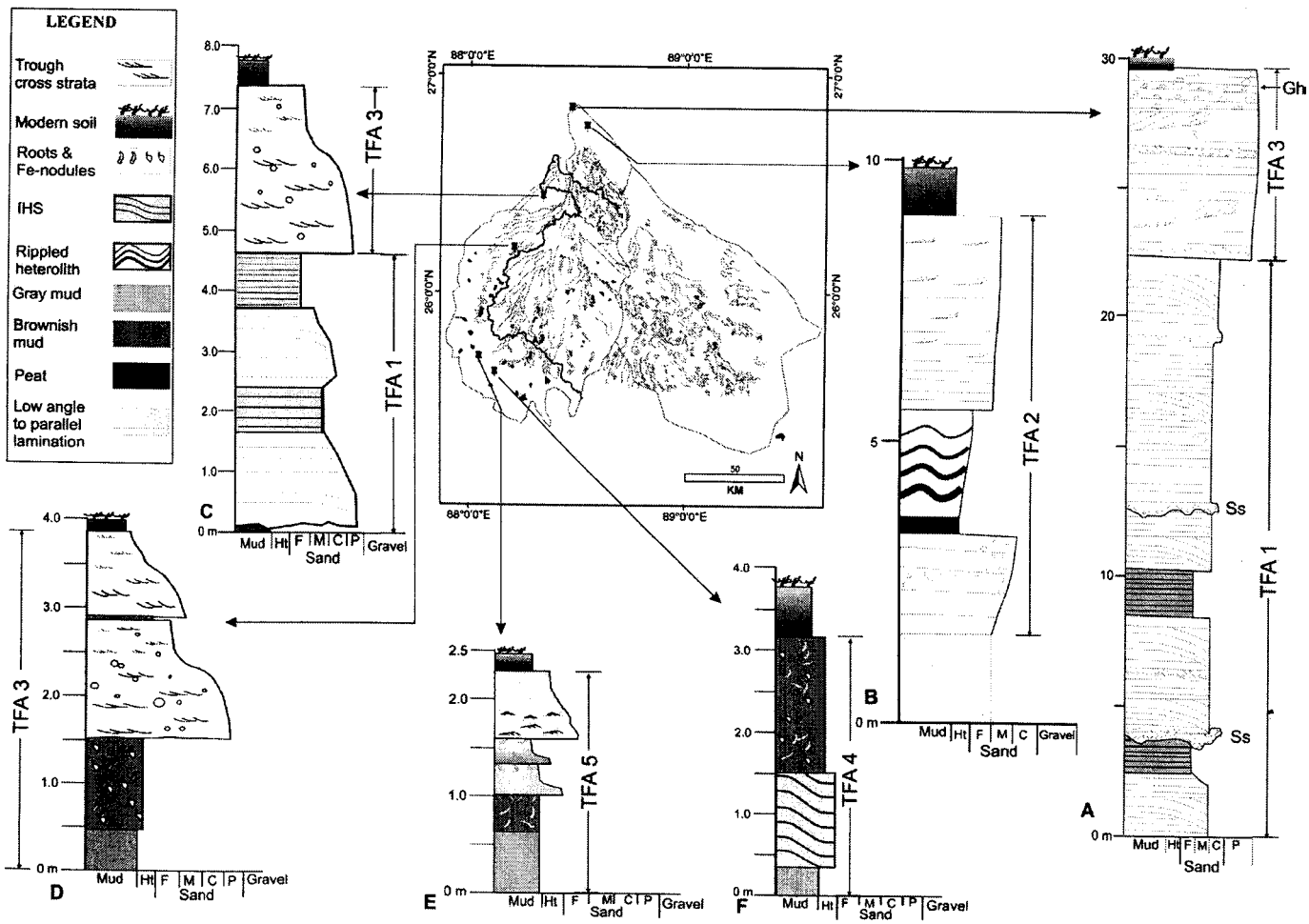

Fig. 8. Sedimentological logs of different sections in lobes 1a, 2 and 3 of the megafan. TFA 1, TFA 2 etc. mark the facies associations. Note sand-dominated deposits in the proximal–medial part of lobes 1a and 3 (log A, C) and increase in the proportion of finer deposits in the distal part of lobes 2 and 3 (log B, E, F). The middle part of the megafan shows sub equal proportion of sandy and muddy deposits (log D).

Table 1
Lithofacies of the Tista megafan deposits.

Facies	Description	Paleocurrent	Occurrences	Interpretation/remark
Stratified sandy pebble gravel (Gh)	Sandy pebble gravel, few cm to 1 m thick, low-angle or horizontally stratified, imbricated clasts		At few places in the proximal part of lobe 2 and top of lobe 3	Traction transported gravel forming gravel sheets near the channel base (Hein and Walker, 1977)
Horizontal to low-angle stratified fine-coarse sand (Sh)	Mm-scale strata occurring in tabular units, few tens of cm thick; laterally traceable for few meters; at places fines upward.	Low-angle strata show SE to S-ward flow	Common in the proximal part of lobe 2 and over a large part of lobe 3	Deposit of upper regime flow probably through migration of very low-amplitude bedforms (Best and Bridge, 1992)
Solitary large planar cross-bedded med.-pebbly sand (Sp)	Isolated sets 30–55 cm thick; foresets at places show sigmoid shape; large clasts occur dispersedly, commonly interlayer with Sh	Few measurement show E to SE flow	Common in the proximal part of lobes 2 and 3.	Large 2-D dunes; at times subjected to transitional to upper flow regime flow allowing transport of pebbles and formation of humpback dunes (Saunderson and Lockett, 1983)
Small trough cross-stratified med. sand (St)	5–20 cm thick sets, forming decimetre scale cosets	Wide dispersion between E and SW	Dominant in medial-distal part of lobes 3 and 2	Small 3-D dunes
Shallow erosional scours (Ss)	10–25 cm deep, up to 5 m wide scours filled with coarse sand to silty sand; show a F–U trend	Broadly to S-ward	Common in proximal as well as distal part of lobe 3	Shallow channel fills
Rippled or massive silt, mud (Fsm)	Dark grey units up to meter thick; massive or with mm-scale laminae marked by alternation of silt-rich and clay-rich layers; wave and current ripple laminations common; iron-encrusted root moulds found locally; at places 10–20 cm thick peat layers.	–	Common in distal part of lobes 2 and 3	Deposition in overbank stagnant pools/marshes with abundant vegetation; occasionally receiving silt-rich crevasse flow and reworked by wind-generated waves
Inclined heterolithic strata of sand–silt–mud (IHS)	Up to 2 m thick inclined strata made up of reddish silt, mud and sand; dip oblique to flow vectors measured from underlying sand (St)	NNW or SSE dip of the IHS	In the distal part of lobe 2	Lateral accretion deposits in mixed-load channels (Thomas et al., 1987)
Brownish red mud with iron-rich nodules and root moulds (Fpr)	Chocolate brown, tough mud units, 0.25 to 1.0 m thick, with abundant iron-rich concretions.	–	In the medial to distal part of lobe 2	Brownish colour, iron-encrusted root moulds and nodules formed in the soil profiles of the megafan surface.

the other megafan deposits described from Ganga Plain (Singh et al., 1993; Shukla et al., 2001) gravelly deposits are virtually absent in the Tista megafan. Similar gravel-free sand- and mud-dominated megafan sediments have, however, been recorded from sub-Andean Camargo Formation of Tertiary age (Horton and Decelles, 2001).

5. Depositional dynamics of the Tista Megafan

Two braided low-sinuosity rivers flank the Tista megafan today, the mountain-fed Tista River, and the foothills-fed Mahananda River. Majority of the presently active channels on the fan surface are plains-fed type. These rivers, fed by ground water and surface run off, are narrower, at places entrenched deeply within megafan deposits, and show much higher sinuosity than either that of the hinterland catchment-fed rivers or that of the paleochannels recognised on the fan surface. The features of the plains-fed streams, particularly their underfit, incised nature, reflect a decreased sediment and water discharge (cf. Sinha and Friend, 1994). The paleochannels, in general, have greater widths and lower sinuosity compared to the modern plains-fed channels (Figs. 2, 3, and 5). Relict mid-channel bars and braided patterns are recognised in the proximal part of some paleochannels of lobe 2 (Fig. 6A). The upstream reaches of these paleochannels are comparable to the size and plan form of modern Tista or Mahananda River. Some of the historical maps as well as archaeological data imply that a radial drainage system comprising Tangan–Atrai–Karatoya once formed large navigable channels directly connected to the Himalayan catchment. Collectively these observations would imply the following: i) During the active aggradation of the Tista megafan possibly much wider braided streams fed by large Himalayan catchments traversed this area. ii) These channels and the megafan have largely been abandoned. The Tista River situated on the eastern margin of the megafan drains the upland catchment basin today, and incises up to 35 m into the megafan deposits of lobe 3. The radial paleodrainage consisting of Tangan–Atrai–Karatoya is now detached from the Himalayan catchments, and like other plains-fed channels is presently incising and reworking the top of the megafan deposits. iii) The paleochannels, as evident from the satellite images and the near-surface sedimentary deposits, were low sinuosity; sandy braided ones near the megafan apex. In the downstream areas, the sinuosity of these channels increased and their sediment load became finer. Floodplain lakes or marshes were common in the distal part of the lobes. Such proximal–distal changes in the paleochannel pattern and its deposits are attributable to decreased slope down the precursor Tista megafan surface.

The observed radiating paleochannel pattern appears to be the combined effect of nodal avulsion of the main channels in the upstream reach and crevasse channel formation in the distal megafan region. Development of crevasses in the downstream part is consistent with increased channel aggradation rate in bank-confined sinuous rivers and is probably reflective of a decreased channel gradient (cf. Mackay and Bridge, 1995; Assine, 2005).

Development of radial sediment lobes and relocation of the trunk channels from the apex are common features in most of the megafans or similar depositional features (Horton and Decelles, 2001; Assine, 2005; Nichols and Fisher, 2007). The existence of radial depositional lobes is also documented from debris-flow dominated or braided stream constructed small, high-gradient, alluvial fans (Bull, 1977; Hubert and Filipov, 1989; Nemec and Postma, 1993). Radial, multi-lobate geometry also characterises many sandy deep-sea fans (Damuth et al., 1988; Reading and Richards, 1994). The sub-aerial

Please cite this article as: Chakraborty, T., Ghosh, P., The geomorphology and sedimentology of the Tista megafan, Darjeeling Himalaya: Implications for megafan building processes, Geomorphology (2009), doi:10.1016/j.geomorph.2009.06.035

Table 2
Facies associations of Tista megafan.

Facies association	Facies	Description and occurrence	Paleocurrent	Interpretation
TFA1	Sh (dominant), Sp, St and rare Gh	Erosively based, 50–90 cm units laterally traceable for more than 15 m; horizontal to low-angle strata grading upward into 10–30 cm muddy silt; rare planar cross-beds and shallow channel fills; 35 m succession in the Tista River shows a coarsening-upward trend; occurrence in the proximal part of lobes 2 and 3.	Varying between 126° and 210°	Unconfined sandy braided stream with flashy discharge and sandy bed load.
TFA 2	St, Sh, Fsm	Up to 3 m thick horizontal or cross-stratified sand units alternate with 15–200 cm thick mud, silt layers with wave and current ripples; thin peat layers at places; common in western and southern margins of lobe 3 and in the medial to distal part of lobe 2.	Mean direction west to southwest	Distal part of the sheet-braided fluvial system lower flow velocity and development of floodplain; wave rippled silt–mud and peats accumulated in floodplain ponds or marshes
TFA 3	St, Sp and Gh (rare) + Fsm, Fpr	1–1.5 m thick, erosively based, coarse, pebbly sand bodies, locally fining upward; horizontal strata, trough cross-strata (5–20 cm) dominates; planar cross-strata (up to 40 cm) also common; few stratified gravel beds in the basal part of the units; overlain by red or grey mud/clay units, at places with iron nodules. Proximal to medial part of lobe 2	Broadly SSW	Braided stream deposits. DA elements not recognised in small exposures but braided bar features are identifiable in satellite images of paleochannels; floodplain fines and incipient soils preserved.
TFA 4	St, IHS, Fsm Fpr	1.5–3.0 fining upwards succession, cross-beds at the base and thick units of fine sand at the top; sand–mud inclined heteroliths comprising 7–32 cm sand layers (with Tg cross-strata) alternating with 3–11 cm mud/clay layers; deep red mud with root moulds and iron concretions common near top. Common in the distal part of lobe 2	Overall paleoflow to SW (220°); observed IHS dip towards NNW or SSE	Mixed-load, meandering streams with well-developed point bars and floodplain fines; soil profiles with abundant root structure common
TFA 5	Dominantly Fsm with thin beds of Fr	2–2.5 m thick dark grey mud and carbonaceous clay with 30–70 cm thick clayey silt beds with ripple lamination; tabular rippled silt beds can be traced laterally for few hundreds meters; few 15–25 cm zones marked by the presence of dense root moulds; these root zones are marked by Fe-enrichment; common in the distal part of lobe 2	–	Large swamp/marsh deposits; clayey rippled beds are probable crevasse lobes encroaching into marshes; rooted horizons represent near emergent surfaces colonized by plants in the marshland.

fans produced in the laboratory or through numerical simulation also show similar multi-lobate form (Whipple et al., 1998; Leeder, 1999; Densmore et al., 2007; Karssenberg and Bridge, 2008). In all these cases fixed channel outlet at the basin margin, lateral unconfinement of the feeder channel as it enters the aggradational basin, high gradient and high sediment load of the main channels appear to control the development of these fan-shaped sediment bodies through random nodal avulsion. The entire surface of the fan-shaped sediment bodies is rarely flooded and deposition at a particular time is confined to a single accretionary lobe. Deposition in a lobe progressively reduces its gradient effecting relocation of the sediment conduit through a nodal avulsion to a site with more favourable gradient. Repetition of this process results in the formation of a fan-shaped sediment body with radial lobes (Schumm et al., 1987; Whipple et al., 1998; Horton and DeCelles, 2001).

A spectrum of sizes, gradients and the depositional processes has been reported from these fan-shaped sediment bodies. Depositional processes operative on these conical, fan-shaped sediment bodies differ significantly in different settings and include sub-aerial debris flow, supercritical sheet flood, turbidity current and fluid-gravity flow. Notwithstanding the difference in depositional processes, size and slope, all these point-sourced conical sediment bodies (fans, megafans, fluvial distributary systems or deep-sea fans) generally share certain common features as discussed above. Occurrence of these features in the Tista megafan implies similar system-scale controls on the development of this megafan. It is generally accepted that there is a complete gradation in the size, slope, sediment load and depositional processes operative on the fan-shaped sediment bodies (cf., Stanistreet and McCarthy, 1993; Nemec and Postma, 1993; Leeder, 1999; Saito and Oguchi, 2005; Hartley et al., 2009). Although occurring at the low-gradient, fine-grained end of a spectrum of conical sediment bodies (cf. Fig. 3 of Blair and McPherson, 1994), the geomorphic features of the Tista megafan outlined above strengthens, the notion of classifying megafans in the 'alluvial fan spectrum'. Although made up entirely of fluvial deposits, megafans as a whole display a distinctive convex-upward cross profile, concave radial profile and radial drainage pattern in contrast to concave-upward cross profiles of the rivers and subparallel orientation of channel network in the alluvial plains (Blair and McPherson, 1994, their Fig. 2). The morphology and sedimentology of the Tista megafan, appear to be more congruent with the classification of alluvial fan spectrum proposed by Stanistreet and McCarthy (1993). In the triangular plot of fan-shaped sedimentary bodies, Stanistreet and McCarthy (1993) proposed, that the debris-flow dominated fans form one end member, the large fan-shaped bodies constructed by braided rivers and low sinuosity/meandering rivers form the other two end-members of the spectrum.

Compared to the postulated continuous, unidirectional shift of the trunk channel across the surface of the Kosi megafan (Mukherjea and Aich, 1963; Gole and Chitale, 1966; Wells and Dorr, 1987; Singh, 1994), the Tista megafan shows multi-lobate geometry with random lobe switching through nodal avulsions. A convincing reason for unidirectional, westward shift of the Kosi River across the megafan surface, particularly up the slope on the eastern half, and the relationship of such this migration with building of the Kosi megafan remains elusive (Wells and Dorr, 1987; Mackay and Bridge, 1995). The latest computer simulation of alluvial systems similar to Kosi megafan has failed to simulate a progressive shift of the channel in one particular direction across a growing fan (Karssenberg and Bridge, 2008; Bridge, personal communication). The megafan studies by earlier workers, on the other hand, appear to demonstrate that unconfinement of the trunk river at

Please cite this article as: Chakraborty, T., Ghosh, P., The geomorphology and sedimentology of the Tista megafan, Darjeeling Himalaya: Implications for megafan building processes, Geomorphology (2009), doi:10.1016/j.geomorph.2009.06.035

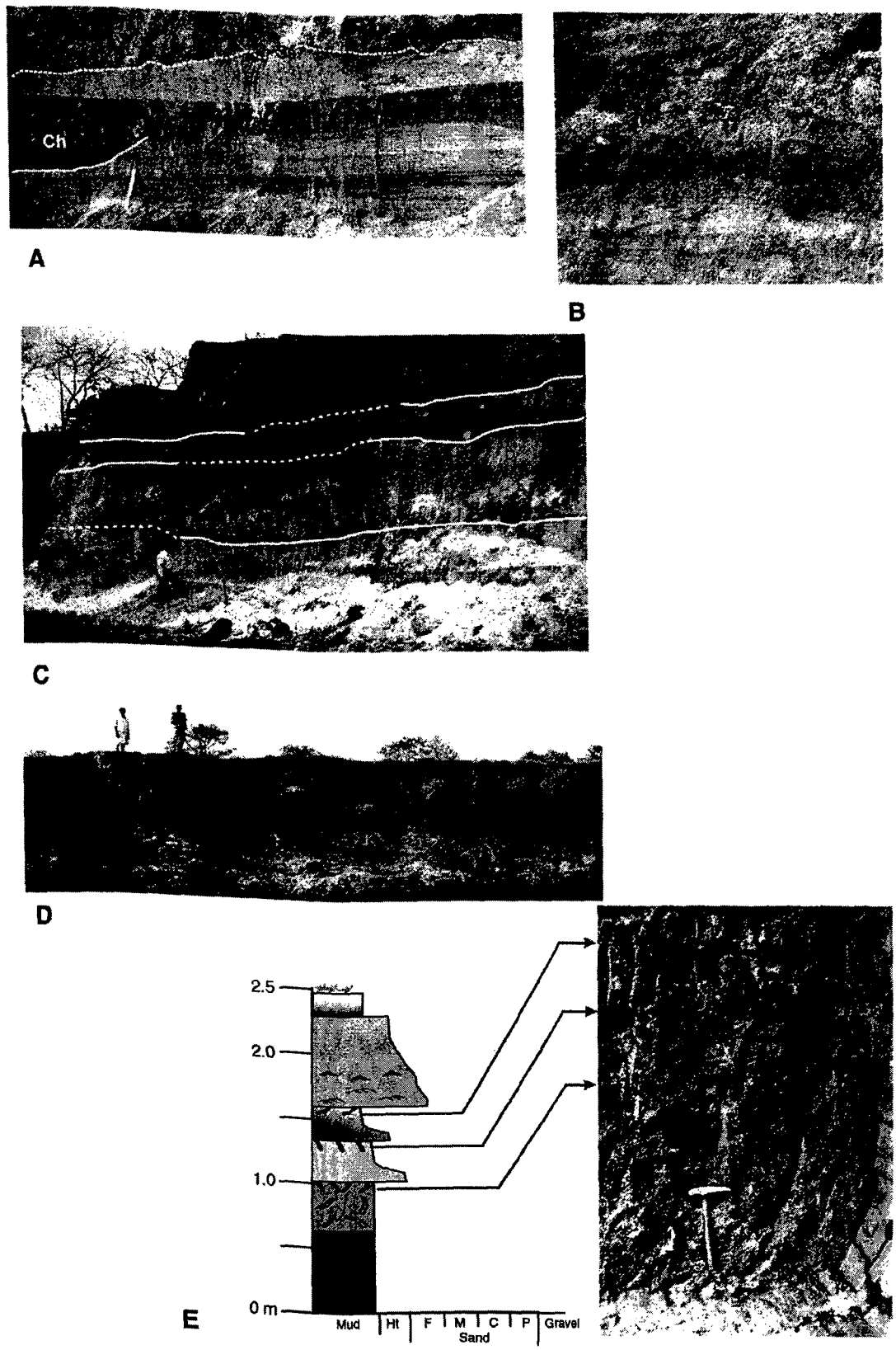

Fig. 9. Sedimentary features of Tista megafan. A. Horizontal strata dominated succession in lobe 3, (log A, Fig. 8). Note shallow erosional scour (Ss) and small channel (Ch). B. Pebbly gravel and gritty cross-stratified sand near the top of lobe 3 succession, Tista River section (log A, Fig. 8). C. Amalgamated sandy channel-fill deposits of TFA 1, Berang River section. Note sheet-like sand bodies. D. A 1.5 m thick inclined heterolithic strata. Photograph looking to SE, Kulik River section (log F, Fig. 8). Note thicker sandy beds in the lower part and deceasing bed thickness and increasing mud up section. E. Log of the marsh deposit exposed in the distal part of lobe 2 (log E, Fig. 8). Photograph shows the close-up of iron-encrusted root zones in the carbonaceous mud deposits.

Please cite this article as: Chakraborty, T., Ghosh, P., The geomorphology and sedimentology of the Tista megafan, Darjeeling Himalaya: Implications for megafan building processes, Geomorphology (2009), doi:10.1016/j.geomorph.2009.06.035

the mountain front, high sediment input and pronounced discharge fluctuations exerts a more fundamental control on megafan building by favouring rapid sedimentation and repeated nodal channel avulsion (Gupta, 1997; Horton and DeCelles, 2001; Leier et al., 2005; Hartley et al., 2009).

6. Conclusions

1. The Tista megafan of the modern sub-Himalayan foreland basin has a surface area of about 18,000 km^2, and is characterised by a radial drainage pattern, a convex-upward cross profile and concave-upward radial profiles. The mean radial gradient of the megafan surface is about 0.05° with a maximum of ~0.19° near its apex.
2. Two hinterland catchment-fed large braided streams, namely the Tista and the Mahananda Rivers, broadly mark the eastern and western margins of the megafan. A network of radial modern channels traverses the megafan, and these channels, compared to the braided Tista and Mahananda, are narrower, more sinuous, plains-fed type and are incised on the megafan surfaces.
3. A radial network of paleochannels is recognised on the satellite images of the megafan. These paleochannels are wider, less sinuous than the modern plains-fed channels and are comparable to hinterland-fed Tista and Mahananda Rivers.
4. Historical maps and archaeological data suggest that until the late eighteenth century many of these modern plains-fed rivers were large navigable channels directly connected to the Himalayan catchments.
5. Three major lobes were recognised on the Tista megafan. The lobes are identified by drainage discordances at their boundaries and their subtle expressions in the cross profiles. Each of the lobes is characterised by radial modern and ancient drainages and down-the-megafan increase in the channel sinuosity. Large vegetated marshes become increasingly common in the distal part of the lobes.
6. Eight facies recognised in the megafan deposits, can be grouped into five facies associations. Sandy sheet-braided stream deposits of Facies Associations 1 and 3 dominate the proximal to medial part of the lobes; the distal parts of the lobes are characterised by low-energy, sand–mud channel deposits of Facies Association 4. The floodplain marsh and/or lake deposits of Facies Associations 2 and 5 become increasingly abundant in the distal part of the lobes. The proximal–distal facies pattern and a radial to southwestward divergent paleoflow observed in the study area are consistent with the geomorphology of the megafan.
7. Existence of a radial, multi-lobate drainage system, convex-up cross profile, concave-up radial profile, and a distinct proximal–distal facies trend recorded from the Tista megafan is similar to the features of many other high-gradient alluvial fans. The morphological similarities in turn may be indicative of the commonness in certain controlling factors between these two depositional systems.
8. The relative age of the lobes inferred in this study indicates repeated and random nodal avulsion of the main feeder channel. In comparison to inferred continuous unidirectional lateral migration of the main feeder channel of the Kosi megafan, accretion and growth through random lobe switching by large mountain-fed streams appear to have controlled the development of the Tista megafan. Similar multi-lobate geometry is common in many other megafans throughout the world.

Acknowledgements

Indian Statistical Institute funded this research. We gratefully acknowledge the help from Rimpal Kar in preparing most of the diagrams and revising them. We appreciate our students, Shyamantak Chatterjee, Samarpan Dey, Jayati Paul and Saunak Basu for various assistances. We are thankful to Bill Dietrich, Leslie Hsu and Trisha Chakraborty for extending all possible help in consulting UC, Berkeley map library. Constructive criticisms and suggestions from reviewers Peter DeCelles, J. A. Fisher, Gary Weissmann and Guest Editor Gary Nichols helped in significantly improving our presentation.

References

Acharrya, S.K., Shastry, M.V.A., 1979. Strtigraphy of the eastern Himalaya. Proc. Himalayan Geology Seminar: GSI Miscl. Publ., vol. 41, pp. 49–64.
Allen, J.R.L., 1983. Studies in fluviatile sedimentation: bars, bar-complexes and sandstone sheets (low sinuosity braided streams) in Brownstones (L Devonian), Wels borders. Sedimentary Geology 33, 237–293.
Arrowsmith, A., 1804. Hindoostan: From Arrowsmith's Map of Asia. David Rumsey Digital Map Collection. University of California, Berkeley.
Arrowsmith, J., 1844. Map of India. World Atlas. David Rumsey Digital Map Collection. University of California, Berkeley.
Assine, M.R., 2005. River avulsions on the Taquari megafan, Pantanal wetland, Brazil. Geomorphology 70, 357–371.
Basu, S.R., Sarkar, S., 1990. Development of Alluvial Fans in the Foothills of the Darjeeling Himalayas and their Geomorphological and Pedological Characteristics. In: Rachocki, A.H., Church, M. (Eds.), Alluvial Fans: A Field Approach. Wiley, Chichester, pp. 321–333.
Bentham, P.A., Talling, P.J., Burbank, D.W., 1993. Braided Stream and Flood-plain Deposition in a Rapidly Aggrading Basin: The Escanilla Formation, Spanish Pyrenees. In: Best, J.L., Bristow, C.S. (Eds.), Braided Rivers: Geological Society of London Special Publication, vol. 75, pp. 177–194.
Best, J.L., Bridge, J.S., 1992. The morphology and dynamics of low-amplitude bedwaves upon upper stage plane beds and preservation of planar laminae. Sedimentology 39, 737–752.
Blair, T.C., McPherson, J.G., 1994. Alluvial fans and their natural distinction from rivers based on morphology, hydraulic processes, sedimentary processes and facies assemblages. Journal of Sedimentary Research A64, 450–489.
Bristow, C., 1999. Gradual Avulsion, River Metamorphosis and Reworking by Underfit Streams: A Modern Example from the Brahmaputra River in Bangladesh and a Possible Ancient Example in the Spanish Pyrenees. In: Smith, N.D., Rogers, J. (Eds.), Fluvial Sedimentology VI International Association of Sedimentologists Special Publication, vol. 28, pp. 221–230.
Bull, W.B., 1977. The alluvial fan environment. Progress in Physical Geography 1, 222–270.
Burbank, D.W., Beck, R.A., Mulder, T., 1996. The Himalayan Foreland Basin. In: Yin, A., Harrison, M. (Eds.), The Tectonic Evolution of Asia. Cambridge University Press, Cambridge, pp. 149–188.
Carry, M., 1811. An Accurate Map of Hindostan or India from Best Authorities. David Rumsey Digital map collection. University of California, Berkeley.
Chakrabarti, D.K., 2001. Mahananda Plains. Archaeological Geography of the Ganga Plain. The Lower and the Middle Ganga. Permanent Black Publishers, Delhi, pp. 58–102.
Collinson, J.D., 1996. Alluvial Sediments. In: Reading, H.G. (Ed.), Sedimentary Environments: Processes, Facies and Stratigraphy. Blackwell Science, Oxford, pp. 37–82.
Damuth, J.E., Flood, R.D., Kowsmann, R.O., Belderson, R.E., Gorini, M.A., 1988. Anatomy and growth pattern of Amazon deep-sea fan as revealed by Long-Range Side-Scan Sonar (GLORIA) and high resolution seismic studies. American Association of Petroleum Geologists Bulletin 72, 885–892.
Dasgupta, S., Pande, P., Ganguly, D., Iqbal, Z., Sanyal, K., Venkatraman, N.V., Dasgupta, S., Sural, B., Harendranath, L., Mazumdar, K., Sanyal, S., Roy, A., Das, L.K., Misra, P.S., Gupta, H., 2000. Sikkim Himalaya and Punea Basin, Plate SEISAT 13. In: Nurula, P.L., Acharrya, S.K., Banerjee, J. (Eds.), Seismotectonic Atlas of India: Kolkata, Geological Survey of India.
Decelles, P.G., Cavazza, W., 1999. A comparison of fluvial megafans in the Cordillarians (Upper Cretaceous) and modern Himalayan foreland basin systems. Bulletin of the Geological Society of America 111, 1315–1334.
Densmore, A.L., Allen, P.A., Simpson, G., 2007. Development and response of a coupled catchment fan system under changing tectonic and climatic forcing. Journal of Geophysical Research 112, F01002, doi:10.1029/2006JF000474, 2007, p. 1–16.
Duchaufour, P., 1982. Pedology. Allen & Unwin, London. 448 pp.
Edinburgh Geographical Institute, 1893. Military Map of Indian Empire. Constable's Hand Atlas of India. Bartholomew, London.
Fielding, C.R., 2006. Upper flow regime sheets, lenses and scour fills: extending the range of architectural elements for fluvial sediment bodies. Sedimentary Geology 190, 227–240.
Geddes, A., 1960. The alluvial morphology of the Indo-Gangetic plain: its mapping and geographical significance. Institute of British Geographers Transactions and Papers 28, 253–276.
Ghosh, P., Chakraborty, C., Chakraborty, T., 2005. Quaternary deposits of the Tista Valley: implications for foredeep sedimentation, tectonism and climate. Abstract Volume, Symposium on "Geoscientific aspects of landscape evolution of North Bengal–Sikkim: environmental problems and developmental perspectives". West Bengal Academy of Science and Technology, pp. 6–7.
Gohain, K., Prakash, B., 1990. Morphology of the Kosi Megafan. In: Rachoki, A., Church, M. (Eds.), Alluvial Fans: A Field Approach. Wiley, Chichester, pp. 151–178.
Gole, C.B., Chitale, S.V., 1966. Inland delta building activity of Kosi River. Journal of the Hydraulics Division, American Society of Civil Engineers HY-2, 111–126.
Goswami, K.G., 1948. Excavations at Bangarh (1938–1941). Ashotosh Museum Memoir No. 1, University of Calcutta, 42 pp & plates I–XXXIII.
Gupta, S., 1997. Himalayan drainage patterns and origin of fluvial megafans in the Ganges foreland basin. Geology 25, 11–14.
Hartley, A.J., Weissmann, G.S., Nichols, G.J., Warwick, G.L., 2009. Distributary fluvial systems: characteristics, distribution and controls on development. Abstract volume, From River to Rock Record – Aberdeen – January 2009, pp. 43–44.

Please cite this article as: Chakraborty, T., Ghosh, P., The geomorphology and sedimentology of the Tista megafan, Darjeeling Himalaya: Implications for megafan building processes, Geomorphology (2009), doi:10.1016/j.geomorph.2009.06.035

Hein, F.J., Walker, R.G., 1977. Bar evolution and development of stratification in the gravely braided Kicking Horse River, British Columbia. Canadian Journal of Earth Sciences 14, 562–570.
Horton, B.K., DeCelles, P.G., 2001. Modern and ancient fluvial megafans in the foreland basin systems of the central Andes, southern Bolivia: implication for drainage network evolution in fold-thrust belts. Basin Research 13, 43–61.
Hubert, J.F., Filipov, A.J., 1989. Debris-flow deposits in the alluvial fans on the west flank of the White Mountains, Owens valley, California, U.S.A. Sedimentary Geology 61, 177–205.
Hunter, W.W., 1876. A statistical account of Bengal, Volume X, Darjeeling, Jalpaiguri & Coochbehar. (First Reprint 1974), D.K. Publishing House, New Delhi.
Huyghe, P., Galy, A., Mugnier, J.L., France-Lanord, C., 2001. Propagation of the thrust system and erosion in the Lesser Himalaya: geochemical and sedimentological evidence. Geology 29, 1007–1010.
Iriondo, M., 1993. Geomorphology and late Quaternary of the Chaco (South America). Geomorphology 7, 289–303.
Karssenberg, D., Bridge, J.S., 2008. A three-dimensional numerical model of sediment transport, erosion and deposition within a network of channel belts, floodplain and hill slope: extrinsic and intrinsic controls on floodplain dynamics and alluvial architecture. Sedimentology 55, 1717–1745.
Lawton, T.F., Boyer, S.E., Schmitt, J.G., 1994. Influence of inherited taper on structural variability and conglomerate distribution, Cordilleran fold and thrust belt, western United States. Geology 22, 339–342.
Leeder, M.R., 1999. Sedimentology and Sedimentary Basins: From Turbulence to Tectonics. Blackwell Science, Oxford. 592 pp.
Leier, A.L., DeCelles, P.G., Pelletier, J.D., 2005. Mountains, monsoons and megafans. Geology 33, 289–292.
Mackay, S.D., Bridge, J.S., 1995. Three-dimensional model of alluvial stratigraphy: theory and application. Journal of Sedimentary Research 65, 7–31.
McKee, E.D., Crossby, E.J., Berryhill, H.L., 1967. Flood deposits, Bijou Creek, Colorado. Journal of Sedimentary Petrology 37, 829–851.
Miall, A.D., 1996. Geology of the Fluvial Deposits. Springer, Berlin. pp. 582.
Mukherjea, Aich, 1963. Sedimentation in the Kosi – a unique problem. Journal of Institution of Engineers (India) 43, 187–198.
Najman, Y., 2006. The detrital record of orogenesis: a review of approaches and techniques used in Himalayan sedimentary basins. Earth Science Reviews 74, 1–72.
Nemec, W., Postma, G., 1993. Quaternary Alluvial Fans in Southwestern Crete: Sedimentation Processes and Geomorphic Evolution. In: Marzo, M., Puigdefabregas, C. (Eds.), Alluvial Sedimentation: Special Publication International Association for Sedimentologists, vol. 17, pp. 235–276.
Nichols, G.J., Fisher, J.A., 2007. Processes, facies and architecture of fluvial distributary system deposits. Sedimentary Geology 195, 75–90.
Perez-Arlucia, M., Smith, N.D., 1999. Depositional patterns following the 1870's avulsion of Saskatchewan River (Cumberland Marshes). Journal of Sedimentary Research 69, 62–73.
Powers, P.M., Lillie, R.J., Yeats, R.S., 1998. Structure and shortening of Kangra Dehra Dun re-entrants, Sub-Himalaya, India. Geological Society of America Bulletin 110, 1010–1027.
Radefeld, C.C.F., 1860. Neueste Karte von Vorder Indien oder Hindostan [electronic resource]/nach den bessten Quellen entworfen und gezeichnet von Radefeld, H., 1844. Hildburghausen ; Philadelphia : Bibliograph. Institut., David Rumsey digital map collection, University of California, Berkeley.
Rajchl, M., Ulycny, D., 2005. Depositional record of an avulsive fluvial system controlled by peat compaction (Neogene, Most Basin, Czech Republic). Sedimentology 52, 601–625.
Ray, N.R., 1980. *Bangalir Itihas* (in Bengali), 3rd Edition, Sakharata Prakasan, Kolkata-700009, 559 pp.
Reading, H.G., Richards, M., 1994. Turbidite systems in deep water basin margins classified by grain size and feeder system. Bulletin of the American Association of Petroleum Geologists 78, 792–822.
Rennel, J., 1794. An Actual Survey of Bengal, Bahar etc. Laurie and Whittle, London.
Saito, K., Oguchi, T., 2005. Slope of alluvial fans in humid regions of Japan, Taiwan and the Philippines. Geomorphology 70, 147–162.
Saunderson, H.C., Lockett, F.P., 1983. Flume Experiments on Bedforms and Structures at the Dune-plane Bed Transition. In: Collinson, J.D., Lewin, J. (Eds.), Modern and Ancient Fluvial Systems: International Association for Sedimentologists, Special Publication, vol. 6, pp. 49–58.
Schumm, S.A., Mosley, M.P., Weaver, W.E., 1987. Experimental Fluvial Geomorphology. Wiley, Chichester. 384 pp.
Shukla, U.K., Singh, I.B., Sharma, M., Sharma, S., 2001. A model of alluvial megafan sedimentation: Ganga Megafan. Sedimentary Geology 144, 243–262.
Singh, R.L., 1994. India: A Regional Geography. National Geographical Society of India, Varanasi, pp. 183–251.
Singh, H., Parkash, B., Gohain, K., 1993. Facies analysis of the Kosi megafan deposits. Sedimentary Geology 85, 87–113.
Sinha, R., Friend, P.F., 1994. River systems and their sediment flux, Indo-Gangetic plains, northern Bihar, India. Sedimentology 41, 825–845.
Stanistreet, I.G., McCarthy, T.S., 1993. The Okavango fan and the classification of the subaerial fan system. Sedimentary Geology 85, 115–133.
Survey of India, 1917. Map of India and Adjacent Countries. Survey of India, Calcutta.
Survey of India, 1924. Map of India. Survey of India, Calcutta.
Thomas, R.G., Smith, D.G., Wood, J.M., Visser, J., Claverly-Range, E.A., Koster, E.H., 1987. Inclined heterolithic stratification – terminology, description, interpretation and significance. Sedimentary Geology 53, 123–179.
Tunbridge, I.P., 1981. Sandy high energy flood sedimentation – some criteria for recognition, with an example from the Devonian of SW England. Sedimentary Geology 28, 70–95.
Wells, N.A., Dorr, J.A., 1987. Shifting of the Kosi River, Northern India. Geology 15, 204–207.
Wesnousky, S.G., Kumar, S., Mohindra, R., Thakur, V.C., 1999. Uplift and convergence along the Himalayan Frontal Thrust, India. Tectonics 18, 967–976.
Whipple, K.X., Parker, G., Paola, C., Mohrig, D., 1998. Channel dynamics, sediment transport, and the slope of alluvial fans: experimental study. Journal of Geology 106, 667–693.
Wilkinson, M.J., Marshall, L.G., Lundberg, J.G., 2006. River behavior on megafans and potential influences on diversification and distribution of aquatic organisms. Journal of South American Earth Sciences 21, 151–172.
Willis, B., 1993. Ancient river systems in the Himalayan foredeep, Chinji Village area, northern Pakistan. Sedimentary Geology 88, 1–76.
Yin, A., 2006. Cenozoic tectonic evolution of the Himalayan orogen as constrained by along-strike variation of structural geometry, exhumation history, and foreland sedimentation. Earth Science Reviews 76, 1–131.

Please cite this article as: Chakraborty, T., Ghosh, P., The geomorphology and sedimentology of the Tista megafan, Darjeeling Himalaya: Implications for megafan building processes, Geomorphology (2009), doi:10.1016/j.geomorph.2009.06.035